Synthesis and Characterization of Transparent Luminescent ZnS:Mn/PMMA Nanocomposites

H. Althues,[†] R. Palkovits,[‡] A. Rumplecker,[‡] P. Simon,[§] W. Sigle,[∥] M. Bredol,[⊥] U. Kynast,[⊥] and S. Kaskel*[,†]

Inorganic Chemistry Department, Technical University of Dresden, Mommsenstrasse 6, D-01069 Dresden, Germany, Max-Planck-Institute of Coal Research, Kaiser-Wilhelm-Platz 1, D-45470 Mülheim a.d. Ruhr, Germany, Max-Planck-Institute for Chemical Physics of Solids, Nöthnitzer Strasse 40, D-01187 Dresden, Germany, Max-Planck-Institut for Metals Research, Heisenbergstrasse 3, D-70569 Stuttgart, Germany, and University of Applied Sciences Münster, Stegerwaldstrasse 39, D-48565 Steinfurt, Germany

Received December 23, 2004. Revised Manuscript Received October 3, 2005

Transparent luminescent nanocomposites were obtained using the bulk polymerization of transparent dispersions containing manganese-doped ZnS nanoparticles with a crystallite size of 2 nm in a mixture of methyl methacrylate and acrylic acid. The effective diameter in the monomer dispersions is 22 nm as determined using dynamic light scattering and depends on the composition of the continuous phase but is significantly higher than the primary crystallite size of the ZnS:Mn nanoparticles initially obtained from the precipitation reaction. The dispersions are stable up to 8 months. Deprotonated carboxylate groups are detected in IR spectra (1547, 1437 cm^{-1}) of particles isolated from a stable dispersion indicating the presence of surface-bound acrylate molecules. Thermal bulk polymerization of the entire dispersions is suitable for production of luminescent acrylic glasses with an emission maximum at 590 nm (330 nm excitation) and a quantum yield of 29.8%. Ultramicrotome cuts of the nanocomposites with a thickness of 50−100 nm were prepared for transmission electron microscopic investigations. In the micrographs, a low degree of agglomeration is observed and the agglomerate diameter is below 20 nm. In the nanocomposites, light scattering and turbidity is minimized due to the small particle size and high degree of dispersion, resulting in highly transparent acrylic glasses with a transmittance as high as 87% (600 nm).

Introduction

The incorporation of inorganic particles into polymers allows one to integrate new functions inside polymer matrixes.[1−7] For transparent plastics, modification of the matrix by dispersing a second inorganic component into the polymer typically results in a significant loss of transparency due to scattering from large particles or agglomerates. A novel approach for the functionalization of transparent plastics is the use of nanoparticles.[8] Since the Rayleigh scattering intensity is proportional to d^6 (d = particle diameter), the integration of small particles (d < 30 nm) can be applied to transparent plastics without dramatic loss of transparency. However, a challenge is to avoid agglomeration inside the matrix, resulting in turbid composites, and thus techniques need to be developed that allow for the integration of particles with a high external surface area into polymers.

In the following, we describe the integration of manganese-doped ZnS nanoparticles (ZnS:Mn) into transparent PMMA (poly(methyl methacrylate)) plastics using an in situ polymerization approach. In the first step, stable ZnS:Mn nanoparticle dispersions are generated in which the monomer forms the continuous phase. In the second step, the continuous phase is polymerized by radical polymerization in substance; i.e., the entire continuous phase is transformed into a solid polymer block (Scheme 1).

Manganese-doped ZnS nanoparticles have been studied by several groups in recent years and synthesis procedures are well-established.[9−16] For Cd(Hg)S(Se,Te) nanoparticles,

* To whom correspondence should be addressed. E-mail: Stefan.Kaskel@chemie.tu-dresden.de. Phone: 49-351-46333632. Fax: 49-351-46337287.
[†] Technical University of Dresden.
[‡] Max-Planck-Institute of Coal Research.
[§] Max-Planck-Institute for Chemical Physics of Solids.
[∥] Max-Planck-Institut for Metals Research.
[⊥] University of Applied Sciences Münster.

(1) Kickelbick, G. *Prog. Polym. Sci.* **2003**, *28*, 83−114.
(2) Beecroft, L. L.; Ober, C. K. *Chem. Mater.* **1997**, *9*, 1302−1317.
(3) Ash, B. J.; Schadler, L. S.; Siegel, R. W. *Mater. Lett.* **2002**, *55*, 83−87.
(4) Avella, M.; Errico, M. E.; Martuscelli, E. *Nano Lett.* **2001**, 213−217.
(5) Godovsky, D. Y. *Adv. Polym. Sci.* **2000**, *153*, 163−205.
(6) Yeh, J. M.; Liou, S. J.; Lin, C. Y.; Cheng, C. Y.; Chang, Y. W. *Chem. Mater.* **2002**, *14*, 154−161.
(7) Popovic, I. G.; Katsikas, L.; Müller, U.; Velickovic, J. S.; Weller, H. *Macromol. Chem. Phys.* **1994**, *195*, 889−904.
(8) Ajayan, P. M.; Schadler, L. S.; Braun, P. V. *Nanocomposite Science and Technology*, 1st ed.; Wiley-VCH: Weinheim, 2003.
(9) Balaz, P.; Valko, M.; Boldizarova, E.; Briancin, J. *Mater. Lett.* **2002**, *57*, 188−191.
(10) Gan, L. M.; Liu, B.; Chew, C. H.; Xu, S. J.; Chua, S. J.; Loy, G. L.; Xu, G. Q. *Langmuir* **1997**, *13*, 6427−6431.
(11) Leeb, J.; Gebhardt, V.; Müller, G.; Haarer, D.; Su, D.; Giersig, M.; McMahon, G.; Spanhel, L. *J. Phys. Chem. B* **1999**, *103*, 7839−7845.
(12) Vacassy, R.; Scholz, S. M.; Dutta, J.; Plummer, C. J. G.; Houriet, R.; Hofmann, H. *J. Am. Ceram. Soc.* **1998**, *81*, 2699−2705.
(13) Xu, S. J.; Chua, S. J.; Liu, B.; Gan, L. M.; Chew, C. H.; Xu, G. Q. *Appl. Phys. Lett.* **1998**, *73*, 478−480.
(14) Konishi, M.; Isobe, T.; Senna, M. *J. Lumin.* **2001**, *93*, 1−8.

10.1021/cm0477422 CCC: $33.50
Published on Web 02/01/2006

Scheme 1. In Situ Polymerization Method for the Generation of Transparent ZnS:Mn/PMMA Nanocomposites

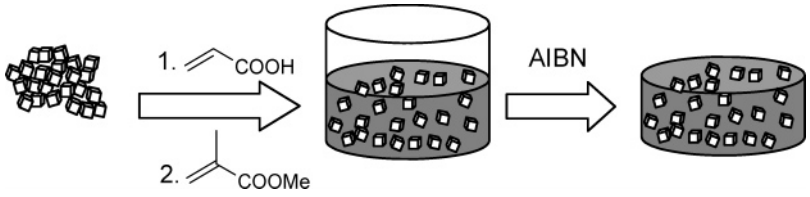

efficient phase transfer into nonpolar solvents is observed after particle capping using thiols or polymer ligands.[17−19] CdSe-based polymer composites were obtained using tri-*n*-octylphosphine oxide[20] or via phase transfer using octadecyl-*p*-vinyl-benzyldimethylammonium chloride.[21] However, cadmium- and mercury-containing additives and phosphine oxides are problematic in industrial polymer processing because they are highly toxic and expensive.

To our knowledge, so far the integration of luminescent ZnS nanoparticles into polymer matrixes was only studied for the manufacture of thin films for electroluminescent devices.[15,22,23] ZnS−polymer nanocomposite films with high refractive index were prepared by incorporating thiophenol-capped ZnS nanoparticles into urethane-based polymers.[24] CdS−ZnS core−shell particles well-dispersed in polycetyl-*p*-vinylbenzyldimethylammonium chloride were obtained using the reverse micelle method.[25]

In thin nanocomposite films ($a < 50\ \mu$m), the small thickness of the film is the reason for the high transmittance. However, in macroscopic acrylate-based glasses ($a > 5$ mm) agglomeration of the particles may lead to a severe loss of the transmittance. Thus, for the development of highly transparent bulk nanocomposites, not only a small particle diameter and narrow particle size distribution are essential but also the key is to develop preparation methods avoiding agglomeration of the particles inside the polymer matrix. The secondary agglomerate structures, present in dried nanoparticle powders, are rarely broken up by direct mixing with polymers in the melt (compounding) or in solution due to the strong interfacial forces and the high specific surface area of inorganic nanoparticles. However, a stable dispersion of the nanoparticles in the monomer can be converted into a transparent nanocomposite if the formation of the polymer in the vicinity of the particles does not induce agglomeration.

In the following, we describe the manufacture of such macroscopic PMMA blocks containing well-separated manganese-doped ZnS nanoparticles (ZnS:Mn) with orange photoluminescence.

Experimental Section

Zinc acetate dihydrate (Fluka, 5.00 g, 22.8 mmol) and manganese acetate tetrahydrate (Fluka, 0.12 g, 0.49 mmol) were dissolved in 150 mL of methanol. Na_2S (Acros, 61%, 3.00 g, 23.3 mmol) dissolved in a mixture of 40 mL of water and 40 mL of methanol was added and the resulting suspension was stirred for 15 min. The white precipitate was separated by centrifugation (4000 rpm, 10 min) and dispersed in acrylic acid (10 g in 30 mL of acrylic acid). Heat treatment at 363 K in air gave a transparent dispersion that was further stabilized by the addition of zinc acetate. Subsequently, the dispersion was diluted with methyl methacrylate (MMA, 200% w/w) and polymerized at 318 K after the addition of AIBN (Acros, 0.2% w/w) for 12 h. Hardening was carried out at 363 K to give a transparent nanocomposite with a ZnS:Mn content of 1.1% w/w.

The transmittance of 5 mm thick PMMA blocks was measured using a UV/Vis-Spectrometer 1650 PC (Shimadzu). Luminescence quantum yields of a 2 mm thick nanocomposite plate and of ZnS:Mn powder isolated from the dispersion in acrylic acid were determined using a 450 W Xe lamp, Acton excitation and emission monochromators of 300 mm focal length and gratings with 1200 g/mm, and an Acton photomultiplier tube P2. Emission spectra were integrated between 500 and 700 nm using an excitation wavelength of 331 nm. Both nanocomposite and powdered sample were evaluated vs LumogenRot F 300 (150 ppm in PMMA, 1.6 mm disk and powdered), with a quantum yield of 42% over the spectral range in question (BASF). LumogenRot F 300 references were generously provided by BASF, Ludwigshafen.

For transmission electron microscopic investigations, one drop of the ZnS:Mn/ AA suspension was placed on a carbon film coated copper grid. After drying, the ZnS:Mn sample was washed with ethanol several times. Transmission electron micrographs were obtained using a Philips CM200 FEG\ST Lorentz electron microscope with a field emission gun at an acceleration voltage of 200 kV.

For further electron microscopic studies the composite material was cut into thin slices by means of an ultramicrotome (element six) (thickness of the sections <100 nm). The slices were supported on holey carbon film covered copper grids. High-angle annular dark-field images (HAADF) were obtained in a VG HB501UX dedicated scanning transmission electron microscope equipped with a cold field-emission gun and operated at 100 kV. HAADF images show bright contrast in areas containing atoms of high atomic number, such as Zn, whereas the light composite matrix (consisting mainly of carbon) shows dark contrast. Therefore, this imaging technique is often referred to as Z-contrast.

For the dynamic light scattering measurements, a Brookhaven instrument (90Plus) was used at 296 K. The viscosity of the MMA-diluted dispersion was 1.13 cP whereas for the acrylic acid dispersion the viscosity of pure acrylic acid was used for the

(15) Kezuka, T.; Konishi, M.; Isobe, T.; Senna, M. *J. Lumin.* **2000**, *87−9*, 418−420.
(16) Igarashi, T.; Isobe, T.; Senna, M. *Phys. Rev. B* **1997**, *56*, 6444−6445.
(17) Gaponik, N.; Talapin, D. V.; Rogach, A. L.; Eychmüller, A.; Weller, H. *Nano Lett.* **2002**, *2*, 803−806.
(18) Potapova, I.; Mruk, R.; Prehl, S.; Zentel, R.; Basche, T.; Mews, A. *J. Am. Chem. Soc.* **2003**, *125*, 320−321.
(19) Koktysh, D. S.; Gaponik, N.; Reufer, M.; Crewett, J.; Scherf, U.; Eychmüller, A.; Lupton, J. M.; Rogach, A. L.; Feldmann, J. *Chem. Phys. Chem.* **2004**, *5*, 1435−1438.
(20) Lee, J.; Sundar, V. C.; Heine, J. R.; Bawendi, M. G.; Jensen, K. F. *Adv. Mater.* **2000**, *12*, 1102−1105.
(21) Zhang, H.; Cui, Z. C.; Wang, Y.; Zhang, K.; Ji, X. L.; Lu, C. L.; Yang, B.; Gao, M. Y. *Adv. Mater.* **2003**, *15*, 777−780.
(22) Yang, Y.; Huang, J. M.; Liu, S. Y.; Shen, J. C. *J. Mater. Chem.* **1997**, *7*, 131−133.
(23) Yang, Y.; Xue, S. H.; Liu, S. Y.; Huang, J. M.; Shen, J. C. *Appl. Phys. Lett.* **1996**, *69*, 377−379.
(24) Lü, C.; Cui, Z.; Wang, Y.; Li, Z.; Guan, C.; Yang, B.; Shen, J. *J. Mater. Chem.* **2003**, *13*, 2189−2195.
(25) Lu, S.-Y.; Wu, M.-L.; Chen, H.-L. *J. Appl. Phys.* **2003**, *93*, 5789−5793.

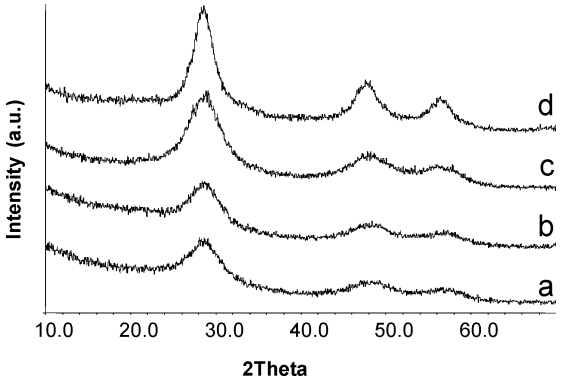

Figure 1. X-ray powder patterns of manganese-doped ZnS nanoparticles obtained by precipitation (molar Zn/S ratio: 4.0 (a), 2.0 (b), 1.3 (c), and 1.0 (d)).

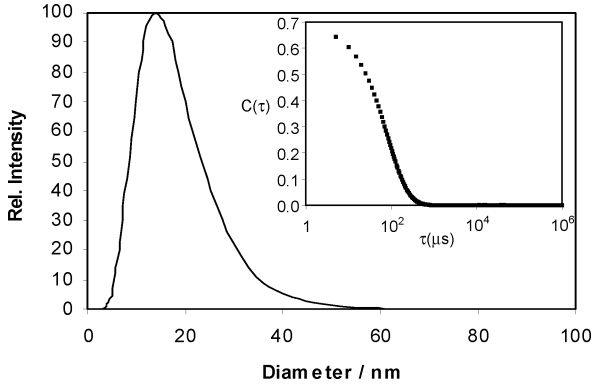

Figure 2. Intensity-weighed particle size distribution of manganese-doped ZnS particles in a monomer dispersion containing methyl methacrylate and acrylic acid (2:1). Inset: corresponding correlation function.

determination of the effective diameter (1.15 cP). All dispersions were filtered using a 0.2 μm PTFE-membrane filter before the measurement.

^{1}H NMR spectra of samples in D_2O were recorded using a Bruker instrument (DPX 300) at 300 MHz and 300 K. A Nicolet instrument (Magna IR 750) was used for Fourier Transform Infrared Spectra measurements in KBr tablets in the range 4000−400 cm^{-1}.

Results and Discussion

Manganese-doped ZnS nanoparticles were obtained from the reaction of Na_2S, zinc acetate and manganese acetate in methanol and isolated via centrifugation.[16] A dependence of the crystallite size with respect to the initial Zn^{2+}/S^{2-} ratio used in the precipitation is evident from the broad Bragg reflections caused by size broadening (Figure 1). The smallest crystallites with a mean diameter of 1.3 nm (line-broadening analysis using the Scherrer equation) are obtained with a high Zn^{2+} excess (molar Zn^{2+}/S^{2-} ratio = 4.0, Figure 1, pattern a), whereas at a ratio of 1.0 the crystallite size is 2.0 nm (Figure 1, pattern d). The concentration of manganese ions does not influence the particle size as much. With the addition of 1 at. % Mn^{2+} relative to Zn^{2+} during synthesis (molar Zn^{2+}/S^{2-} ratio = 2.0), the resulting particle diameter is 1.6 nm, while 10% Mn^{2+} leads to particles 1.9 nm in diameter. According to Bol et al.,[26] the quantum efficiency of ZnS:Mn nanocrystals reaches a maximum for doping levels of 1.5−5.6% and is constant in this range. However, the optimum concentrations depend strongly on synthesis conditions.[26] In this work a doping concentration of 2.1 at. % Mn^{2+} was chosen, leading to 1.0 at. % incorporated Mn^{2+} ions, as determined by elemental analysis.

Dispersion of Luminescent ZnS:Mn Nanoparticles in Acrylic Acid and MMA. The key step for the generation of transparent plastics is to transfer the particles into a stable dispersion of the monomer. ZnS cannot be directly dispersed in MMA without severe agglomeration, leading to an unstable dispersion. In our approach, the particles are first agitated in acrylic acid (AA) at higher temperature, leading to a stable, transparent dispersion of the nanosized particles. This concentrated dispersion can be diluted with organic solvents or other comonomers such as methyl methacrylate. The size of the particles in the AA/MMA dispersion (1:2) was determined using dynamic light scattering (Figure 2).

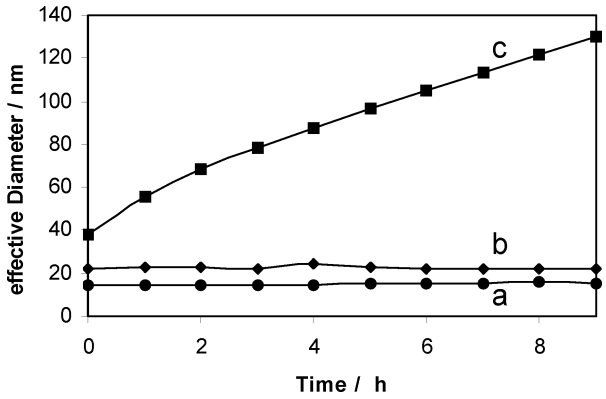

Figure 3. Effective diameter of manganese-doped ZnS particles in dispersions of (a) acrylic acid, (b) methyl methacrylate and acrylic acid (2:1), and (c) acetone and acrylic acid (5:1).

Typically, a broad size distribution is obtained with a mean particle size of 22 nm and a polydispersity index of 0.16. The tail toward larger diameters is caused by aggregates of primary particles. The stability of the dispersions was monitored for several hours using dynamic light scattering. Figure 3a shows the average particle size in the pure acrylic acid dispersion as a function of time. The effective diameter is 14 nm and does not significantly change within several hours. In fact, the pure acrylic acid dispersion is stable over more than 8 months! The acrylic acid dispersion can be diluted with up to 200% methyl methacrylate without loss of transparency. In the AA/MMA dispersion the effective particle diameter is 22 nm and also constant for 8 h (Figure 3b). In comparison to the crystallite size determined from size broadening using the Scherrer equation (above), the effective diameter determined from light scattering differs by a factor of 10. Transmission electron micrographs of ZnS:Mn nanoparticles, taken from the dispersion in acrylic acid, confirm the presence of single, isolated nanocrystals (Figure 4, inset). The overview image (Figure 4) shows layers of uniform particles, but does not allow for determination of the degree of aggregation. Within the limits of error of the different methods, the comparison indicates that crystallite and agglomerate size in the dispersion are not identical. Thus, the higher effective diameter observed by means of dynamic light scattering indicates a low degree of agglomeration, even in transparent dispersions. However, the small agglomerates in the dispersions are stable at room temperature for several months.

(26) Bol, A. A.; Meijerink, A. *J. Phys. Chem. B* **2001**, *105*, 10197−10202.

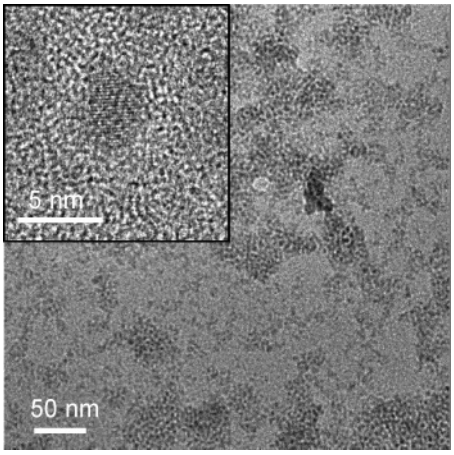

Figure 4. Transmission electron micrograph of ZnS:Mn nanoparticles isolated from dispersion in acrylic acid. Inset: High-resolution image of a single nanocrystal.

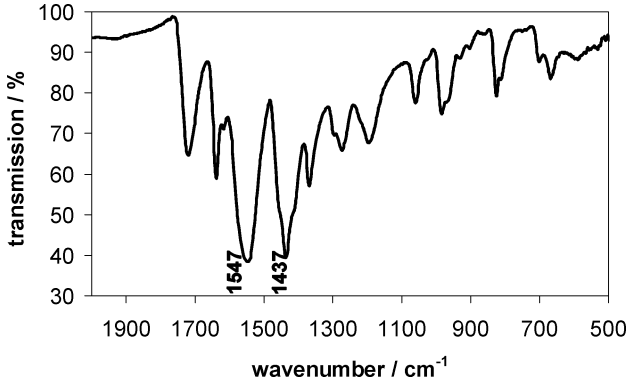

Figure 5. IR spectrum of manganese-doped ZnS nanoparticles isolated from an acrylic acid dispersion.

In contrast, for a dispersion diluted with acetone, a steady increase of the effective diameter up to 130 nm after 9 h is observed (Figure 3c) that is not accompanied by crystal growth according to XRD powder patterns, demonstrating a delicate dependence of the dispersion stability on chemical composition. The stability of monomer dispersions and the possibility to dilute such dispersions with a second monomer such as MMA is crucial for the subsequent bulk polymerization used in our approach to obtain acrylic glasses.

To preclude the formation of poly(acrylic acid) during the heat treatment, which could also be responsible for the stability of the dispersion, we have analyzed the continuous phase using ^{1}H NMR. However, in solution only the dimerization product was detected as a minor impurity. The particles were subsequently isolated from the acrylic acid dispersion by adding methanol and separating the solid precipitate. The precipitate was dissolved in a mixture of DCl and D_2O. In the resulting solution, only monomeric acrylic acid was detected, indicating that the small molecules are responsible for effective stabilization of the particles in the dispersion. In IR spectra of ZnS:Mn nanoparticles, isolated after the acrylic acid treatment, bands at 1547 and 1437 cm^{-1} confirm the presence of deprotonated carboxyl groups that are coordinated to the surface of the ZnS particles (Figure 5).[15] Adsorbed acrylic acid molecules are known to increase the photoluminescence intensity of ZnS:Mn nanocrystals.[15]

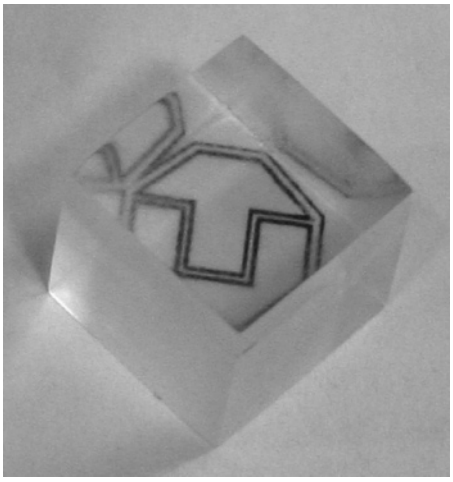

Figure 6. Photograph of a transparent ZnS:Mn/PMMA nanocomposite block ($10 \times 10 \times 10$ mm^3) obtained using in situ bulk polymerization.

The stability of the dispersion is critically affected by several factors. In particular, small amounts of primary amines or water stabilize the dispersion; especially octylamine prevents aggregation when unpolar solvents such as MMA are added to the dispersion of particles in acrylic acid. The addition of zinc salts such as zinc acetate or zinc acrylate enhances the stability, while sodium acrylate or magnesium acetate do not stabilize the dispersion. Thus, adsorption of ions and subsequent electrostatic stabilization seems to be crucial for the stabilization. The latter is surprising since the zeta potential of inorganic particles in nonpolar solvents is typically very small.[27] Electrophoretic mobility measurements of the ZnS/AA-MMA dispersion were below detectability. Only if the acrylic acid dispersion is diluted with acetone, low mobilities (-1.02×10^{-8} $m^2/V{\cdot}s$) can be detected, corresponding to a zeta potential of -18 mV.

Thus, two factors are responsible for the stability of the ZnS/monomer dispersion: (1) coordination of acrylic acid modifies the surface of the particles and leads to a hydrophobization; (2) the adsorption of ions leads to a surface charge and causes electrostatic repulsion.

In Situ Polymerization and Nanocomposite Properties. Transparent composites are obtained by polymerization in the bulk. Bulk polymerization is industrially used for the production of acrylic glasses and PMMA with high molecular weight. As compared to other polymerization techniques in solvents, in our bulk polymerization approach the entire continuous phase is transformed into a solid block. The blocks are highly transparent. Even 10 mm thick blocks do not appear turbid (Figure 6). To achieve this goal, the dispersion also has to be stable at the polymerization temperature for at least 8 h until most of the monomer is converted. The glasses obtained are insoluble in organic solvents and show only a low degree of swelling in contact with solvents. A shrinkage of 17% compared to the volume of the liquid dispersion was observed for the nanocomposites after polymerization.

Since the crystallite size of the luminophor is 1.3−2.0 nm and the particles are only little agglomerated in the dispersion and in the composite (below), the transmittance of the

(27) Morrison, I. D. *Colloid Surf. A* **1993**, *71*, 1−37.

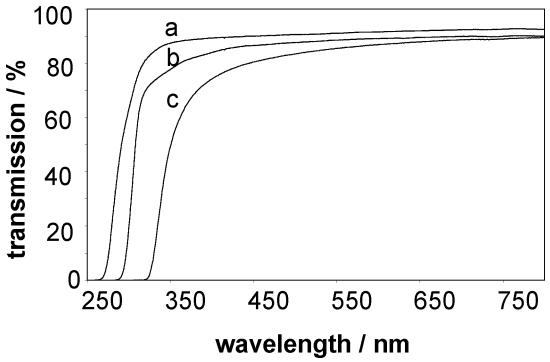

Figure 7. Transmission spectra of (a) pure PMMA, (b) PAA/PMMA copolymer, and (c) ZnS:Mn/PMMA nanocomposite.

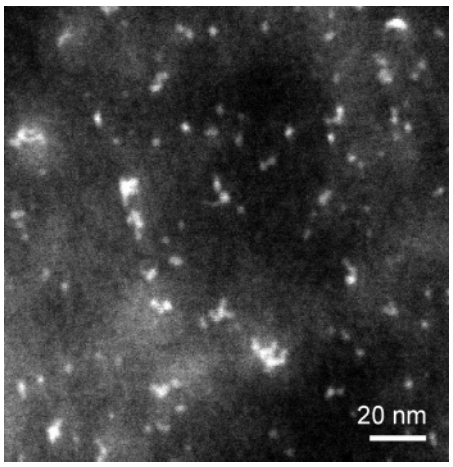

Figure 8. Scanning transmission electron micrograph of the ZnS:Mn/PMMA nanocomposite (ultramicrotome cut).

composites is very high (Figure 7). Pure PMMA has a transmittance of 92% (Figure 7a). The loss of 8% is caused by reflection on the two surfaces of the block (5 mm thickness). In our approach, significant amounts of acrylic acid are copolymerized with MMA. The transmittance of the pure copolymer blocks (MMA:AA = 2:1) is somewhat lower than that of PMMA (89.1%, λ = 600 nm) (Figure 7b). The final ZnS/AA-MMA nanocomposite contains acrylic acid and small amounts of zinc acetate. Larger particles would give rise to a significant reduction of the transmittance, whereas in the nanocomposite (Figure 7c) the transmittance is still as high as 87.3% (600 nm).

The high transmittance confirms the concept of our approach. The integration of nanoparticles allows for the incorporation of functional inorganic particles that are invisible by the human eye. Thus, novel functions can be realized that may not be achieved by modification of functional polymer branches alone. An advantage of inorganic phosphors is the high UV stability, whereas organic molecules are prone to bleaching. However, long-term stability tests are beyond the scope of this work.

A representative scanning transmission electron micrograph of the nanocomposite is shown in Figure 8 (ultramicrotome cut, thickness < 100 nm). The particles are highly dispersed in the composites. Due to the small size of the crystallites (1.3−2 nm) and the presence of the matrix, we were unable to obtain atomic resolution TEM data. In addition, at high electron dose rate, typically the organic ultramicrotome cut was not stable. In the scanning transmission electron micrograph (Z-contrast), the particles appear as white inclusions slightly larger than the primary crystallite size determined from line broadening. A low degree of agglomeration is detected. Most of the agglomerates are below 5 nm in diameter but also extended structures with a length up to 20 nm are discerned. As compared to the effective diameter in the dispersion (22 nm) determined using dynamic light scattering, the agglomerates observed by STEM in the composite are slightly smaller. However, a direct comparison of the results is problematic since size distributions from DLS are intensity-weighed whereas those from STEM are number-weighed. Additionally, the degree of agglomeration in the dispersion is not necessarily identical with that in the nanocomposite.

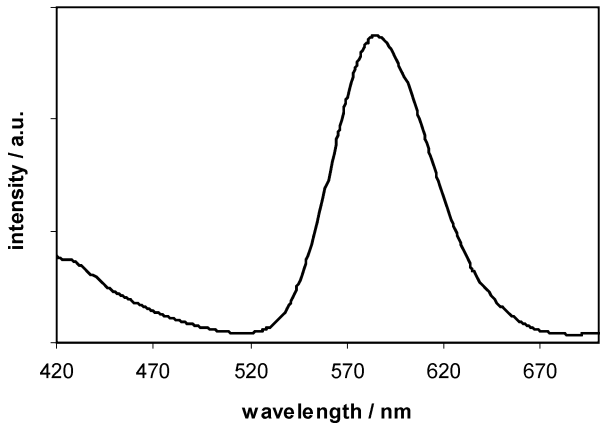

Figure 9. Emission spectrum of the ZnS:Mn/PMMA nanocomposite (330 nm excitation).

Through all processing steps, the functionality of the ZnS:Mn nanoparticles is fully retained. The composites show the orange luminescence of the Mn-doped nanoparticles when irradiated with UV light (254 nm). The emission spectrum (330 nm excitation) of the composite (Figure 9) shows the same broad band as bulk ZnS:Mn centered at 590 nm.[15] The emission band at 420 nm can be attributed to trap emission of ZnS and fluorescence of acrylic acid.[15] For the determination of quantum efficiencies the emission range of 500−700 nm and an excitation wavelength of 331 nm were used. A quantum efficiency of 29.8% was determined for the nanocomposite (2 mm thick plate) while a higher value of 38% was measured for the isolated ZnS:Mn powder. The deviation between nanocomposite (transmission) and powder (reflectance) quantum yields of 8% is very reasonable, considering the very low reflectance of the reference LumogenRot at 331 nm.

Conclusion

We have presented an efficient method for the generation of luminescent inorganic−organic hybrid materials. Whereas other methods for the synthesis of inorganic nanoparticles often make use of highly toxic and expensive stabilizing agents such as phosphine oxides, amines, thiols, and surfactants, the method presented here is highly cost efficient and may be suitable for industrial production.

Acknowledgment. This research project is funded by the "Young Scientist Nanotechnology Initiative" of the Federal Ministry of Education and Research (BMBF: FK 03X5502).

CM0477422